Since January 2020 Elsevier has created a COVID-19 resource centre with free information in English and Mandarin on the novel coronavirus COVID-19. The COVID-19 resource centre is hosted on Elsevier Connect, the company's public news and information website.

Virus Research 192 (2014) 34–45

Contents lists available at ScienceDirect

Virus Research

journal homepage: www.elsevier.com/locate/virusres

Transmissible gastroenteritis virus and porcine epidemic diarrhoea virus infection induces dramatic changes in the tight junctions and microfilaments of polarized IPEC-J2 cells

Shanshan Zhao, Junkai Gao, Liqi Zhu, Qian Yang*

Key Lab of Animal Physiology and Biochemistry, Ministry of Agriculture, Nanjing Agricultural University, Wei gang 1, Jiangsu, PR China

ARTICLE INFO

Article history:
Received 23 May 2014
Received in revised form 15 August 2014
Accepted 19 August 2014
Available online 27 August 2014

Keywords:
Porcine epidemic diarrhoea virus
Transmissible gastroenteritis virus
IPEC-J2 cells
Tight and adherens junctions
Microfilaments
MAPK

ABSTRACT

Viral infection converts the normal constitution of a cell to optimise viral entry, replication, and virion production. These conversions contain alterations or disruptions of the tight and adherens junctions between cells as part of their pathogenesis, and reorganise cellular microfilaments that initiate, sustain and spread the viral infections and so on. Using porcine epidemic diarrhoea virus (PEDV), transmissible gastroenteritis virus (TGEV) and a model of normal intestinal epithelial cells (IPEC-J2), we researched the interaction between tight and adherens junctions and microfilaments of IPEC-J2 cells with these viruses. In our work, the results showed that IPEC-J2 cells were susceptible to TGEV and PEDV infection. And TGEV could impair the barrier integrity of IPEC-J2 cells at early stages of infection through down-regulating some proteins of tight and adherens junctions, while PEDV cloud cause a slight of damage in the integrity of epithelial barrier. In addition, they also could affect the microfilaments remodelling of IPEC-J2 cells, and the drug-interfered microfilaments could inhibit viral replication and release. Furthermore, PEDV + TGEV co-infection was more aggravating to damage of tight junctions and remodelling of microfilaments than their single infection. Finally, the PEDV and TGEV infection affected the MAPK pathway, and inhibition of MAPK pathway regulated the changes of tight junctions and microfilaments of cells. These studies provide a new insight from the perspective of the epithelial barrier and microfilaments into the pathogenesis of PEDV and TGEV.

1. Introduction

Porcine epidemic diarrhoea virus (PEDV) and transmissible gastroenteritis virus (TGEV) are members of the *Coronaviridae* family (Sestak and Saif, 2002). They both replicate in the differentiated enterocytes covering the villi of the porcine small intestine (Kim and Chae, 2003) and cause acute enteritis in swine of all ages, which is characterised by vomiting, diarrhoea, and dehydration; the mortality rate in seronegative suckling piglets may reach 100% (Chae et al., 2000). Despite the similar clinical diseases and lesions induced, PEDV and TGEV are distinct viral entities. PEDV is unable to grow in porcine cell cultures permissive to the growth of TGEV, such as PK15 cells, and is more closely related to the human respiratory coronavirus HCoV 229E than to TGEV according to the amino acid sequence of the membrane protein (Kim et al., 1999).Enterocytes are connected to each other to form a barrier that separates the inside of the organism from its environment. Essential components of this epithelial fence are the tight and adherens junctions (TJs and AJs) (Cereijido et al., 2008). Some pathogens use tight junction proteins as receptors for their attachment and subsequent internalisation, such as Hepatitis C virus (HCV) and reoviruses (Evans et al., 2007; Guglielmi et al., 2007). Infectious enteric agents that alter tight junctions often elicit inflammatory cascades and cause diarrhoea. Rotaviruses are a major cause of viral gastroenteritis leading to diarrhoea and morbidity in mammals. Its VP8 protein alters the localisation of claudin-3, ZO-1 and occludin, which consequently leads to disruption of the barrier integrity of tight junctions during their infection (Nava et al., 2004). TGEV and PEDV also cause severe diarrhoea in piglets, but it is not known whether this is related to damage to the TJs and AJs of epithelial cells.In addition, TJs and AJs use a variety of transmembrane proteins linked to the microfilaments and to intracellular signalling molecules (Etournay et al., 2007; Gonzalez-Mariscal et al., 2008). Following the changes to TJs and AJs, the microfilaments of the host cell are often co-opted by viruses at many stages of their life cycle,

* Corresponding author. Tel.: +86 02584395817; fax: +86 02584398669.
E-mail address: zxbyq@njau.edu.cn (Q. Yang).

http://dx.doi.org/10.1016/j.virusres.2014.08.014
0168-1702/

such as attachment, internalisation, endocytosis, nuclear targeting, replication, assembly, or cell-to-cell spread. Viruses induce rearrangements of microfilaments so that they can utilise them as tracks or move them aside when they represent barriers. Viral particles recruit molecular motors in order to hitchhike rides to different subcellular sites which provide the proper molecular environment for uncoating, replicating and packaging viral genomes (Burckhardt and Greber, 2009; Vaughan et al., 2009). However, there are few reports about the interactions of PEDV and TGEV with microfilaments of host cells.Mitogen-activated protein (MAP) kinases are Ser/Thr protein kinases that respond to extracellular stimuli such as growth factors and stress, among others. Previous studies have shown that the MAPK signalling pathway cannot only up- or down-regulate the expression of several TJ proteins to alter the molecular composition within TJ complexes, but also plays an important role in microfilament remodelling (Gerits et al., 2007; Melamed et al., 1995).To clearly answer the questions of whether PEDV and TGEV infection could impair the tight and adherens junctions of epithelial cells, how interactions with PEDV, TGEV and microfilaments of epithelial cells occur, and how to change the proteins in the MAPK signalling pathway, we used PEDV and TGEV to infect the porcine intestinal epithelial cell line (IPEC-J2). Results showed that both PEDV and TGEV could infect IPEC-J2 cells, and that they could also down-regulate certain proteins of tight and adherens junctions to alter the epithelial barrier integrity. In addition, they affected the polymerisation and depolymerisation of microfilaments in IPEC-J2 cells, and the disordered microfilaments could also suppress the replication and release of these viruses. Furthermore, PEDV + TGEV co-infection enhanced the damage to tight junctions and the remodelling of microfilaments. Finally, PEDV and TGEV infection impacted on activation of the MAPK signalling pathway in IPEC-J2 cells, and MAPK inhibitor could affect the tight junctions and microfilaments of cells.

2. Materials and methods

2.1. Cell lines and culture

The IPEC-J2 cells (Liu et al., 2010) were donated by Zhanyong Wei from Henan Agricultural University (Henan Province, Zhengzhou, China). ST (pig testis cell line) and Vero (African green monkey kidney cell line) cells were provided by Jiangsu Academy of Agricultural Sciences (JAAS, Jiangsu Province, Nanjing, China). IPEC-J2 cells were cultured and maintained in RPMI 1640 medium (Gibco, USA), supplemented with 7% foetal calf serum (FBS; Gibco, USA), penicillin (100 IU/ml), and streptomycin (100 mg/ml) (Invitrogen, USA). Vero and ST cells were cultured in Dulbecco modified Eagle's medium (Gibco, USA), supplemented with 5% foetal bovine serum, penicillin (100 IU/ml), and streptomycin (100 mg/ml) solutions.

TGEV (STC3 strain) (He et al., 2001), PEDV (CV777 strain) (Brian and Baric, 2005) were also provided by JAAS. TGEV was propagated in ST cells and PEDV was propagated in Vero cells; these were purified as described by Hofmann and Wyler (1988).

Confluent monolayers of IPEC-J2 cells were inoculated with TGEV at a multiplicity of infection (MOI) of 0.1, PEDV at an MOI of 0.1, and PEDV + TGEV both at an MOI of 0.1 for 1 h at 37 °C. Then, the inoculums and unattached viruses were removed and fresh growth medium was added. Infected cells were analysed after the required incubation period.

2.2. Immunofluorescence staining

To examine whether the PEDV/TGEV infected the IPEC-J2 cells, the TGEV-, PEDV-, TGEV + PEDV-infected and mock-infected cells at 0, 6, 12, 24, 48, 72 h post-infection (pi) were determined by indirect immunofluorescence. All group cells grown on glass cover slips in 24-well tissue culture plates were fixed with 3.7% polyoxymethylene, washed 3 times with 0.1 M PBS and permeabilised for 5 min with 0.1% Triton X-100. The cells were incubated with a 1% solution of BSA (30 min, room temperature, RT), then stained with FITC-conjugated TGEV polyclonal antibody (VMRD, USA) and monoclonal mouse anti-PEDV M protein (a gift of Zhang Zhi ban, Harbin Veterinary Research Institute, China) respectively (overnight, 4 °C in dark conditions). Following washing 5 times with 0.1 M PBS, a Cy3-conjugated sheep anti-mouse IgG (A0521, Beyotime, China) was added to the cells (1:400,1 h, RT). The negative control slices were treated in an identical manner except the primary antibodies were omitted. Cells were washed 3 times with 0.01 M PBS and images were acquired using a fluorescence microscope (Zeiss, Germany).

To examine the effects of PEDV/TGEV on the cytoskeletal organisation of IPEC-J2 cells, all groups at 0, 20, 40 minpi, and 1, 2, 12, 24, 48, 96 hpi, were stained with FITC-Phalloidin and determined by immunofluorescence. In short, washed infected cells were fixed with polyoxymethylene, and permeabilised for 5 min with 0.1% Triton X-100. The cells were incubated with a 1% solution of BSA (30 min, RT), and stained with FITC-Phalloidin (30 min, RT, in dark conditions). Images were acquired using a fluorescence microscope (Zeiss, Germany).

2.3. Virus titration assay

TGEV-, PEDV-infected and mock-infected cells were seeded onto 6-well plates (5×10^5) and cultured for 2, 6, 12, 24, 48, 72 h. TGEV and PEDV were collected by freezing and thawing the plates three times, and determined by the tissue culture infectious dose 50 ($TCID_{50}$) in ST and Vero cells, respectively.

2.4. Transepithelial electrical resistance (TEER) assay

TEER, a measure of tight junctions (TJ) integrity, is measured by epithelial tissue volt-ohmmeter (Millicell ERS-2, Millipore Corporation, USA) as described previously (Shatos et al., 1992). In short, IPEC-J2 cells were seeded on 24 collagen-coated Millicell filter inserts with a 0.4 mm pore size (Millipore, USA). When the IPEC-J2 cells reached confluence and were infected TGEV/PEDV at an m.o.i. of 0.1. TEER was calculated from the measured potential difference between the apical and basolateral sides of the cell layer by epithelial tissue volt-ohmmeter. All cells were measured in real-time. Resistance is expressed as both $\Omega\,cm^2$ and percent original TEER value relative to a control:

$$\text{Normal resistance}(\Omega\,cm^2) = (\text{TEER1} - \text{blank}) \times 0.33\,cm^2$$

(for 24 well Millicell Filter)

2.5. Permeability measurements

Permeability was determined by measuring the paracellular passage of 4 kDa fluorescein isothiocyanate dextran (FITC-dextran) (Sigma–Aldrich, USA) dissolved in HBSS (1 mg/ml, Gibco, USA). IPEC-J2 cells were seeded on 24 well collagen-coated Millicell filter inserts with a 0.4 mm pore size (Millipore, USA). After the IPEC-J2 cells reached confluence and infected TGEV/PEDV at an MOI of 0.1. To measure flux in the apical to the basolateral direction, 200 μl of the FITC-dextran tracer solution was loaded onto the apical side of the monolayer and cells were incubated for 20, 40 or 60 min at 37 °C. After this period, 100 μl of the solution was measured for the tracer concentration in the basolateral compartment using a BioTek fluorescence/absorbance microplate reader at an excitation wavelength of 492 nm and emission of 520 nm.

2.6. Western blotting

At 20, 40, 60 minpi and 24 hpi, the PEDV-, TGEV-, PEDV + TGEV-infected and mock-IPEC-J2 cells were harvested and prepared for Western blot, as described by McBride and Machamer (2010). Polyclonal anti-occludin, polyclonal anti-claudin-1, monoclonal anti-ZO-1, and monoclonal anti-E-cadherin (Invitrogen, USA) were used at a dilution of 1:1000 in 5% BSA in TBST and HRP-conjugated anti-rabbit IgG or anti mouse IgG diluted 1:10,000 in 5% non-fat dry milk in TBST. The SDS gel was transferred to 0.4 μm PVDF membrane (Millipore, USA) and detection with SuperSignal WestPico (Pierce, Thermo, USA). Western blotting was quantified by Quantity One (Quantity One® 1-D Analysis Software 170-9600, Bio-Rad).

2.7. Transmission electron microscope

TGEV-, PEDV-, TGEV + PEDV-infected and mock-infected cells were harvested by 0.25% trypsinisation (Sigma, USA) and then fixed in a 2.5% glutaraldehyde solution in PBS for 24 h. After fixation, the monolayer was gently removed from the flask with a rubber policeman and the cell suspension was pelleted by low speed centrifugation (2500 × *g* for 5 min). The cells were then washed twice by centrifugation in 0.1 M PBS. The pellet of cells was then fixed overnight at 4 °C for further standard treatment for transmission electron microscope (TEM), as described by Pontefract et al. (1989).

2.8. Effects of the microfilament inhibitor on PEDV and TGEV infection

Microfilament inhibitors, Jas (jasplakinolide, Enzo Life Sciences, Switzerland) and Cyto D (cytochalasin D, Gibco, USA), could interfere with the polymerisation and depolymerisation of the microfilaments in cells. Firstly, in order to study the effects of microfilament disorder on PEDV and TGEV entry, monolayer IPEC-J2 cells were pre-treated with RPMI medium containing Jas (0.2 μM) or Cyto D (2 μM) for 1 h at 37 °C. IPEC-J2 cells were inoculated with TGEV, PEDV, and PEDV + TGEV at an MOI of 0.1 for 1 h at 37 °C, respectively. The unattached viruses were removed and the infected IPEC-J2 cells were collected for analysing $TCID_{50}$ or detecting the level of viral RNA by quantitative RT-PCR (qRT-PCR). Secondly, in order to study the effects of microfilament disorder on PEDV/TGEV release, monolayer IPEC-J2 cells were inoculated with TGEV, PEDV, and PEDV + TGEV at an MOI of 0.1 for 1 h at 37 °C, respectively. The unattached viruses were removed and incubated with RPMI medium. Then the Jas (0.2 μM) or Cyto D (2 μM) was added to the infected cells from 6 to 9 hpi, the supernatants and the infected IPEC-J2 cells were collected for analysing $TCID_{50}$ or detecting the level of viral RNA by qRT-PCR. Finally, in order to study the effects of microfilament disorder on virus replication and release, monolayer IPEC-J2 cells were inoculated with TGEV, PEDV, and PEDV + TGEV at an MOI of 0.1 for 1 h at 37 °C, respectively. The unattached viruses were removed and incubated with RPMI medium containing Jas (0.2 μM) or Cyto D (2 μM) was added to the infected cells from 1 to 9 hpi, only the infected IPEC-J2 cells were collected for analysing $TCID_{50}$ or detecting the level of viral RNA by qRT-PCR.

2.9. Quantitative real-time PCR (qRT-PCR)

Total RNA was extracted using a commercial kit (TaKaRa, Japan). Then, RT-PCR was performed using an RT-PCR kit (TaKaRa, Japan) according to the manufacturer's instructions. To determine the gene expression profiles, individual samples were diluted 1:10 and 2 μl was amplified in a 20 μl reaction containing 10 μl of SYBR Premix™ Ex Taq (TaKaRa), 0.4 μl of ROX dye II and 0.4 μM of each of the forward and reverse gene-specific primers using an ABI 7500 instrument (Applied Biosystems, USA). PEDV M gene was one target gene (GenBank accession no. AF353511.1), and the primers were: FP: 5′-aggtctgcattccagtgctt-3′, RP: 5′-ggacatagaaagcccaacca-3′. TGEV M gene was another target gene (GenBank accession no. AF302262.1), and the primers were: FP: 5′-gtgcttcctctcgaaggtgt-3′, RP: 5′-cccatccagtcgcactactt-3′. Porcine GAPDH gene was used as the internal parameter (GenBank accession no. NM_001206359.1). The primers were: FP: tcatcatctctgccccttct, RP: gtcatgagtccctccacgat. The data were analysed using the ABI PRISM 7500 software tool (Applied Biosystems, USA). 7500 Real-Time PCR System (ABI) and Fast-Start Universal SYBR Green Master (Takara) were used for qRT-PCR. Amplification conditions were 95 °C for 10 min, followed by 40 cycles of 95 °C for 30 s and 60 °C for 60 s. Each sample and negative controls (no template) were run in at least three technical replicates. GAPDH was amplified under the same conditions as internal control to normalise reactions. After completion of the PCR amplification, the relative fold change was calculated based on the $-\Delta\Delta ct$ calculation.

2.10. FACS analysis

PEDV-, TGEV- and PEDV + TGEV-infected and mock-infected IPEC-J2 cells at 1 and 24 hpi were harvested by 0.25% trypsinisation, then fixed and permeabilised in FACS permeabilisation buffer II (BD Pharmingen, USA), washed 3 times with 0.01 M PBS and incubated with a 1% solution of BSA (30 min, RT). Then, cells stained with the primary antibodies anti-ERK1/2 antibody, anti-ERK1/2 (phospho T202 + Y204) antibody, anti-p38 antibody, anti-p38 (phospho T180 + Y182) antibody, anti-JNK1 + JNK2 antibody and anti-JNK1 + JNK2 (phospho T183 + Y185) antibody (Abcam, Hong Kong) were incubated overnight at 4 °C. Subsequently, cells were washed 3 times with 0.01 M PBS and the PE-conjugated goat anti-rabbit IgG2b (Invitrogen, USA) was added (1 h, RT). The negative control cells were treated in an identical manner, except the primary antibodies were omitted. Cells were then washed, and 1×10^4 cells were analysed by flow cytometry for the mean fluorescence intensity (MFI). The results are expressed as the mean fluorescence intensity ratio. The mean fluorescence intensity ratio was calculated using the formula: $(MFI_{\text{infection phospho protein}}/MFI_{\text{infection total protein}})/(MFI_{\text{control phospho protein}}/MFI_{\text{control total protein}})$.

2.11. Effects of MAPK pathway inhibitor on PEDV and TGEV infection, the tight junctions and microfilaments of IPEC-J2 cells

In order to study the effects of MAPK pathway of IPEC-J2 cells on PEDV and TGEV infection, the tight junctions and microfilaments of IPEC-J2 cells, the monolayer IPEC-J2 cells were pre-treated with RPMI medium containing 50 μm/l of ERK-MAPK-specific inhibitor (PD98059), 10 μm/l of p38-MAPK-specific inhibitor (SB203580) or 10 μm/l of JNK-MAPK-specific inhibitor (SP600125) for 2 h at 37 °C. IPEC-J2 cells were inoculated with TGEV, PEDV and PEDV + TGEV at an MOI of 0.1 for 1 h at 37 °C, respectively. The unattached viruses were removed and the infected IPEC-J2 cells were cultured with RPMI medium containing those three inhibitors for the required time. The analysis of mock and treated IPEC-J2 cells is as follows: (1) Mock and treated IPEC-J2 cells at 12 and 24 hpi were added Trizol to detect the level of viral RNA by qRT-PCR. (2) Mock and treated IPEC-J2 cells at 60 minpi and 24 hpi were harvested and prepared for Western blot, as described in Section 2.6. (3) Mock and treated IPEC-J2 cells at 40, 60 minpi and 12, 24 hpi were fixed with 3.7% polyoxymethylene and stained with FITC-Phalloidin for immunofluorescence, as described in Section 2.2.

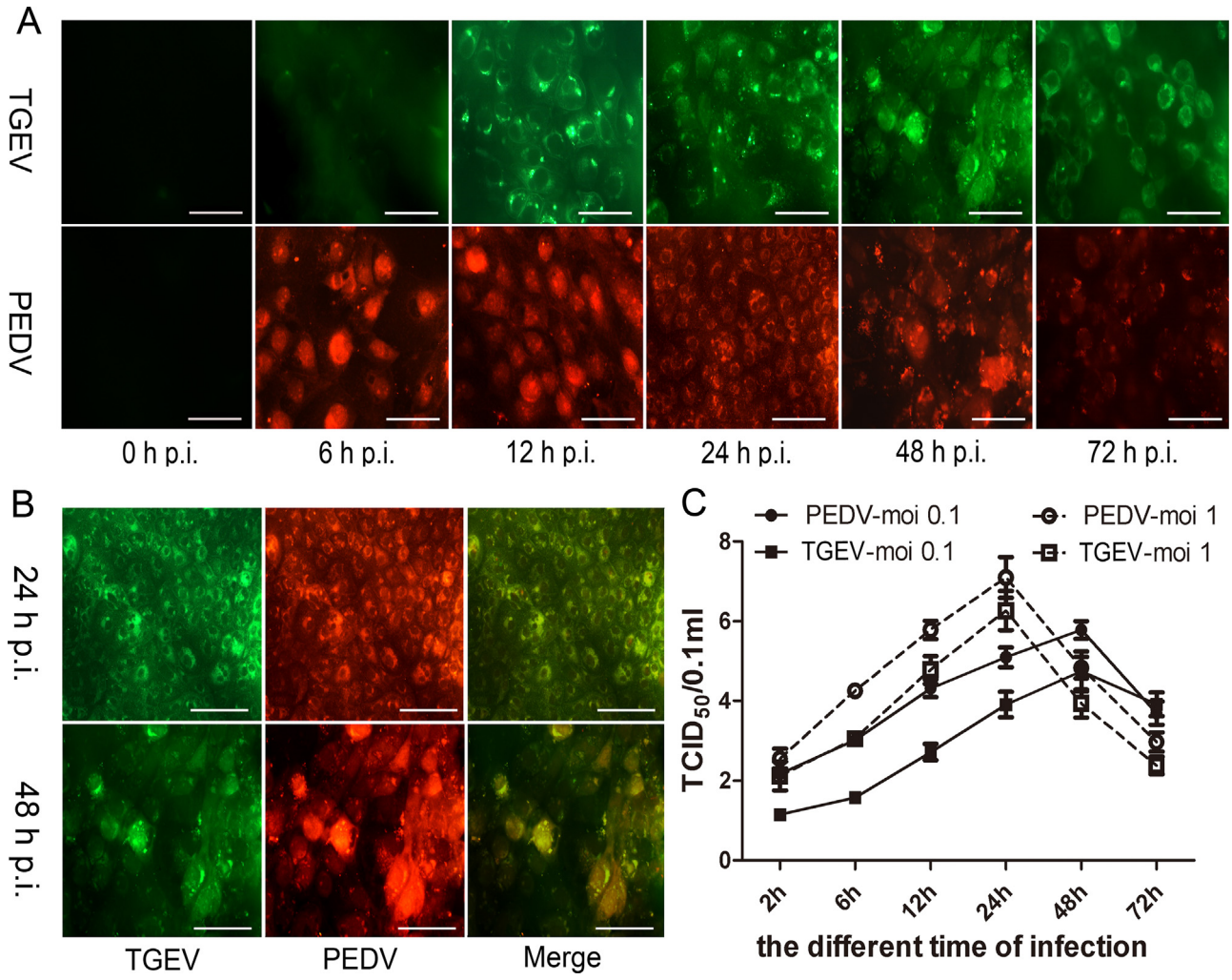

Fig. 1. PEDV and TGEV infected IPEC-J2 cells. (A) Immunofluorescence images of TGEV (green) and PEDV (red) infected IPEC-J2 cells at 0, 6, 12, 24, 48, 72 h post-infection (pi). Scale bars represent 40 μm. (B) Fluorescent images of PEDV + TGEV co-infected IPEC-J2 cells at 24 and 48 hpi. Scale bars represent 40 μm. (C) The viral titres of TGEV and PEDV infected IPEC-J2 cells at 2, 6, 12, 24, 48 and 72 hpi. Data express the mean ± SEM ($n = 3$). (For interpretation of the references to color in text, the reader is referred to the web version of this article.)

2.12. Statistical analysis

The statistical analysis was performed using the Statistical Product and Services Solutions (SPSS) package, version 16.0. Duncan's test was conducted to determine the differences among treated groups. The means of paired groups were analysed by ANOVA. Significance was indicated by a probability of $p < 0.05$.

3. Results

3.1. IPEC-J2 cells are susceptible to PEDV and TGEV

Firstly, to determine whether PEDV and TGEV could infect and replicate in IPEC-J2 cells, IPEC-J2 infected at an MOI of 0.1 PEDV and TGEV at 0, 6, 12, 24, 48, 72 h post infection (pi) were observed by immunofluorescence staining. From the results, both PEDV and TGEV could infect the IPEC-J2 cells. After PEDV infection 6 h and TGEV infection 12 h, the immunofluorescences were read visually from images. Initially, the immunofluorescences were distributed in the plasma membrane, then in the cytoplasm. The above phenomenon might because the two viruses were first distributed in the plasma membrane, then they increased in the cytoplasm from 12 to 24 hpi. Finally, these viruses decreased in the cytoplasm over time due to lack of nutrients for the IPEC-J2 cells (Fig. 1A). Similarly, the phenomenon of PEDV or TGEV single infection was consistent with their co-infection (Fig. 1B). To study the percentage of PEDV and TGEV infected IPEC-J2, $TCID_{50}$ was used to draw the viral proliferation curve. In the early infection (6 hpi), the titre of TGEV replication was lower than PEDV. At 24 hpi, although both TGEV and PEDV reached the replication peak, the titre of TGEV replication was still lower than the PEDV. The data showed that the same concentration of TGEV and PEDV infected the IPEC-J2 cells, the PEDV replication was faster that TGEV. Moreover, the higher the concentration of virus was, the faster the virus replication was to reach the peak. These data showed that MOI 1 of PEDV and TGEV infection reached a peak at 24 hpi, while the MOI 0.1 of their infection reached a peak at 48 hpi and then gradually decreased (Fig. 1C).

3.2. PEDV and TGEV infection instantly destroyed the epithelial barrier integrity

To assess whether PEDV or TGEV single infection or co-infection could damage the epithelial barrier of IPEC-J2 cells, we first measured the changes in the transepithelial electrical resistance (TEER) of IPEC-J2 cells infected with them. From the results, we observed that the TEER of the control group (mock group) maintained in the 3500 $\Omega\,cm^2$ from 0 to 84 hpi, while the TEER of IPEC-J2 cells infected with PEDV declined at 20 minpi, restored after 40 min,

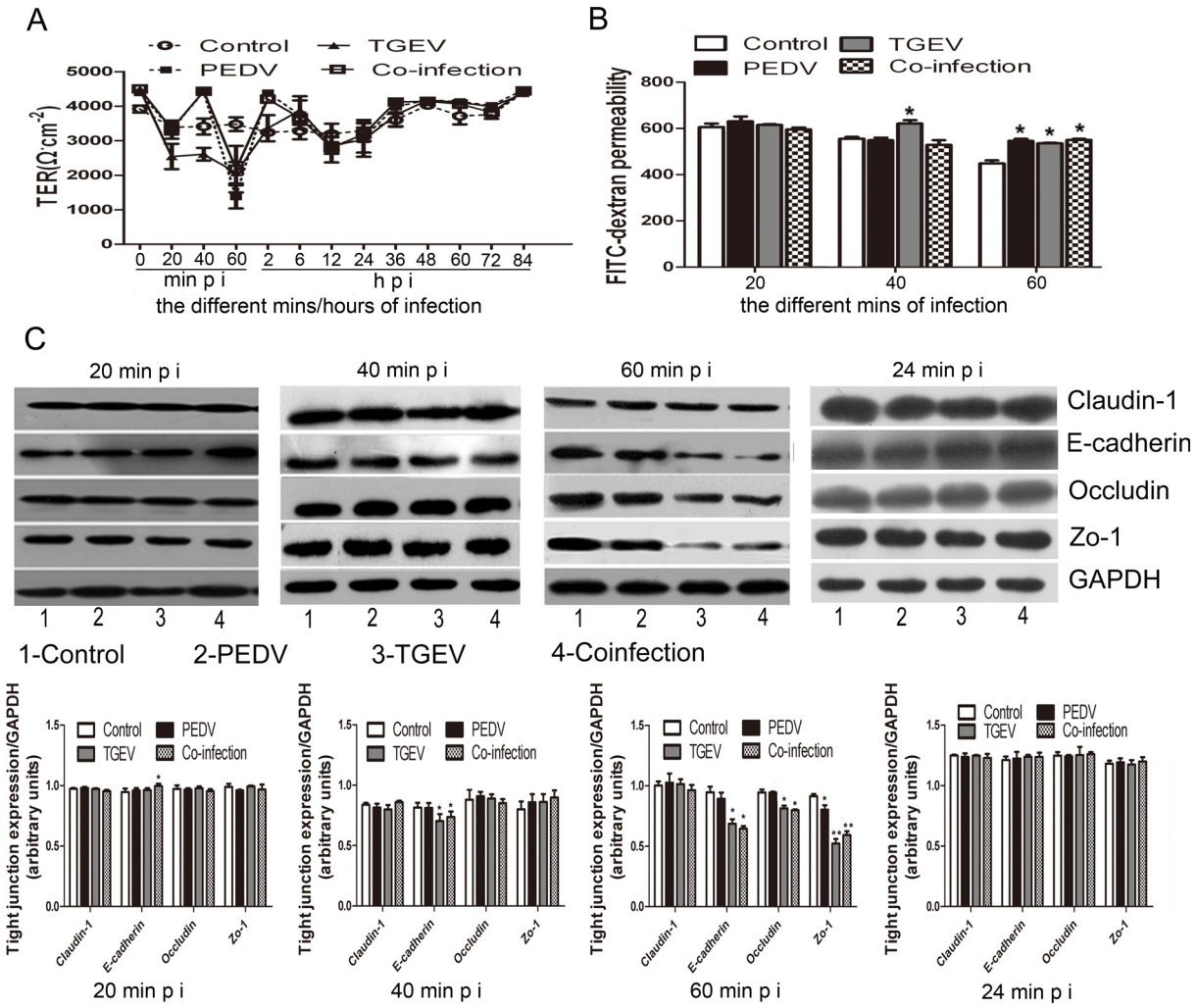

Fig. 2. The integrity of the epithelial barrier is impaired by PEDV and TGEV infection. (A) Transepithelial electrical resistance (TEER) of PEDV-, TGEV- and PEDV + TGEV-infected IPEC-J2 cells from 0 to 84 hpi. Data express the mean ± SEM ($n = 3$). (B) Paracellular permeability of PEDV-, TGEV- and PEDV + TGEV-infected IPEC-J2 cells at 20, 40 and 60 minpi. Data express the mean ± SEM ($n = 3$). The symbol * indicates statistically significant differences ($P < 0.05$) when compared with the control group, and the symbol ** indicates statistically very significant differences ($P < 0.01$) when compared with the control group. (C) The expression of Claudin-1, E-cadherin, Occludin and ZO-1 in PEDV-, TGEV- and PEDV + TGEV-infected IPEC-J2 cells at 20, 40, 60 minpi and 24 hpi was analysed via western blotting. The intensity of the bands in terms of political density was measured and normalised against GAPDH expression. Data express the mean ± SEM ($n = 3$). The symbol * indicates statistically significant differences ($P < 0.05$) when compared with the control group, and the symbol ** indicates statistically very significant differences ($P < 0.01$) when compared with the control group.

declined again after 60 min, and restored again at 2 hpi. TEER then remains more or less unchanged. Compared with the control group, TGEV single infection or co-infection decreased gradually from 20 to 60 min and reached the lowest value at 60 min, especially in the case of their co-infection. Then, levels all gradually restored and remained unchanged from 2 to 84 h (Fig. 2A). Finally, the TEER in TGEV and/or PEDV infected IPEC-J2 cells were unchanged compared with control group from 84 to 120 hpi, gradually decreased from 132 to 204 hpi that might be due to the IPEC-J2 cells death (Additional Fig. 1). To further study whether the permeability of epithelial cells infected with PEDV, TGEV and PEDV + TGEV were changed from 20 to 60 minpi, we measured the passage of a macromolecule, FITC-dextran, across these virus-infected IPEC-J2 monolayer cells grown on Transwell membranes. The permeability of IPEC-J2 infected with TGEV at 40 minpi was higher than other groups ($p < 0.05$) and the above permeability at 60 minpi was also significantly increased compared to the control group ($p < 0.05$) (Fig. 2B). To further investigate whether tight and adhesion junctions proteins played an important role in the instantaneous destruction of the epithelial barrier integrity at 20, 40, 60 minpi and 24 hpi, we measured the three important tight junction proteins claudin-1, occluding and ZO-1 and an adhesion junction protein E-cadherin in the PEDV-, TGEV-infected and their co-infected IPEC-J2 cells. The results demonstrated that the expression of E-cadherin in the PEDV + TGEV-infected IPEC-J2 cells at 20 minpi was higher than the control group and PEDV infected group ($p < 0.05$). Moreover, the expression of E-cadherin in the TGEV-infected and PEDV + TGEV-infected IPEC-J2 cells at 40 minpi were notably lower than other groups ($p < 0.05$). The expression of E-cadherin, Occludin and ZO-1 in the TGEV infected- and PEDV + TGEV-infected IPEC-J2 cells was lowest at 60 minpi ($p < 0.01$). Finally, claudin-1, occluding, ZO-1 and E-cadherin were unchanged in TGEV, PEDV-infected and PEDV +TGEV-infected IPEC-J2 cells compared with the control group at 24 hpi ($p > 0.05$). All of the results demonstrated that TGEV and TGEV + PEDV co-infection could instantaneously impair the integrity of epithelial barrier at early stages of infection, and then gradually return back to normal levels. In addition, ZO-1, Occludin and E-cadherin played

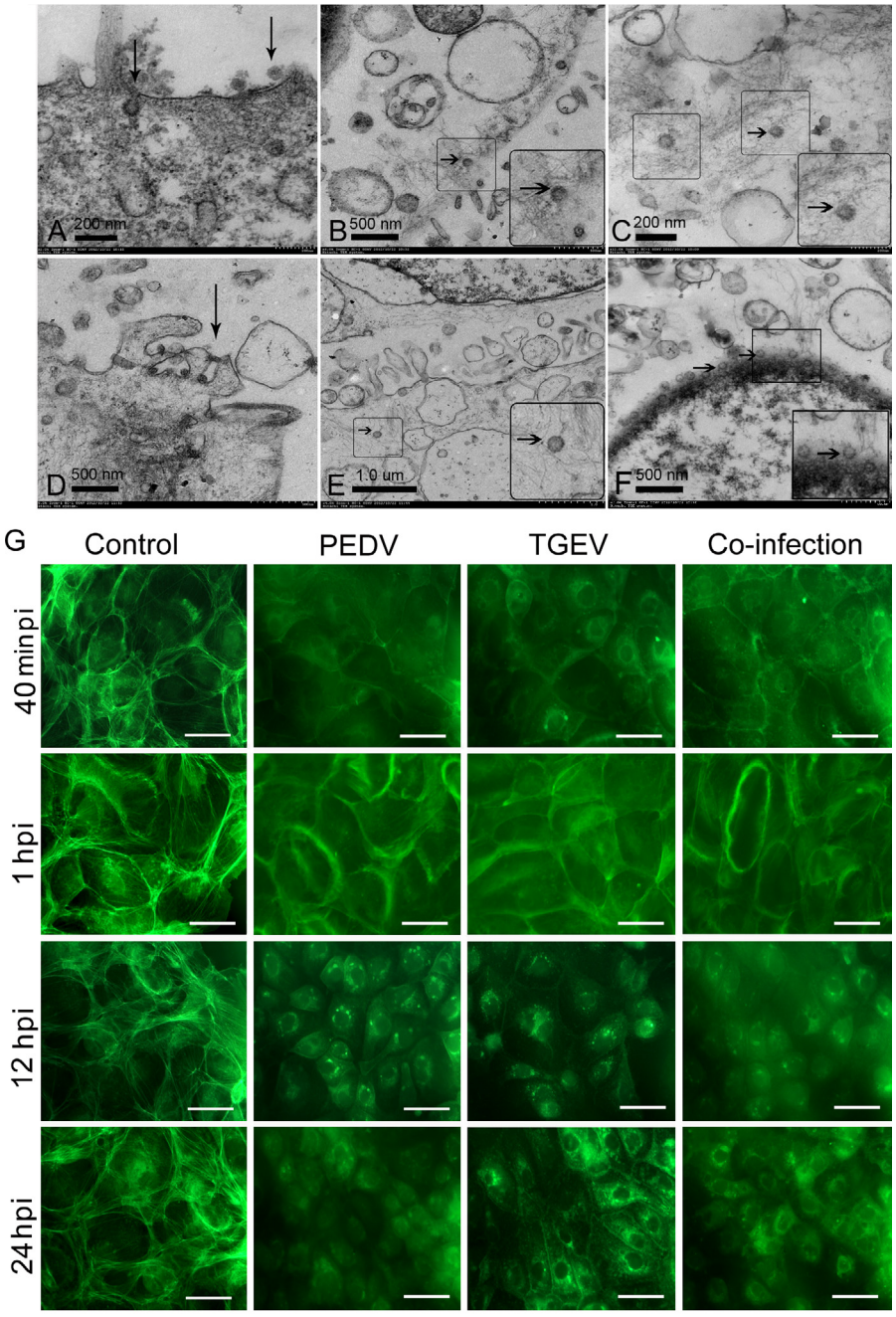

Fig. 3. Alteration of microfilaments of PEDV- and TGEV-infected IPEC-J2 cells. Transmission electron micrographs of microfilaments of IPEC-J2 cells infected with PEDV (A–C) and TGEV particles (D–F) at 24 hpi. (E) Many microfilaments gathered around the PEDV, and appeared to be auxiliary to form membrane vesicles for wrapping the virus when the PEDV absorbed the plasma membrane. (F) In the cytoplasm, a large number of microfilaments gathered around the PEDV, suggesting that the movement of viruses relies on the microfilaments. (G) Immunofluorescence images of microfilaments in PEDV-, TGEV- and PEDV + TGEV-infected IPEC-J2 cells at 40 minpi and 1, 12, 24 hpi were stained with FTTC-phalloidin. Scale bars represent 10 μm.

important roles in the barrier function changes of TGEV and their co-infected IPEC-J2. However, PEDV single infection only could cause a slight of damage in integrity of epithelial barrier.

3.3. The attachment, entry and release of PEDV and TGEV were dependent on the microfilaments

There is a clear evidence that numerous tight and adhesion junction proteins can directly interact with the microfilaments, and the reestablishment of the microfilaments plays a crucial role during viral attachment, entry, replication and release (Avota et al., 2011). We hypothesised that the life cycle of PEDV and TGEV were also dependent on the microfilaments. From the results of TEM, PEDV and TGEV moved along the filopodia which are formed by microfilaments and moved towards the cells (Fig. 3A). Many microfilaments gathered around the PEDV, and appeared to be auxiliary to form membrane vesicles for wrapping the virus when the PEDV absorbed the plasma membrane (Fig. 3A and B). In the cytoplasm, a large number of microfilaments gathered around the PEDV, suggesting that the movement of viruses relies on the microfilaments (Fig. 3C). The same phenomena were also seen in the TGEV infected (Fig. 3D–F) and PEDV + TGEV co-infected IPEC-J2 cells (pictures not shown), and we also observed the virus binding the microfilaments in the nuclear membrane (Fig. 3D).

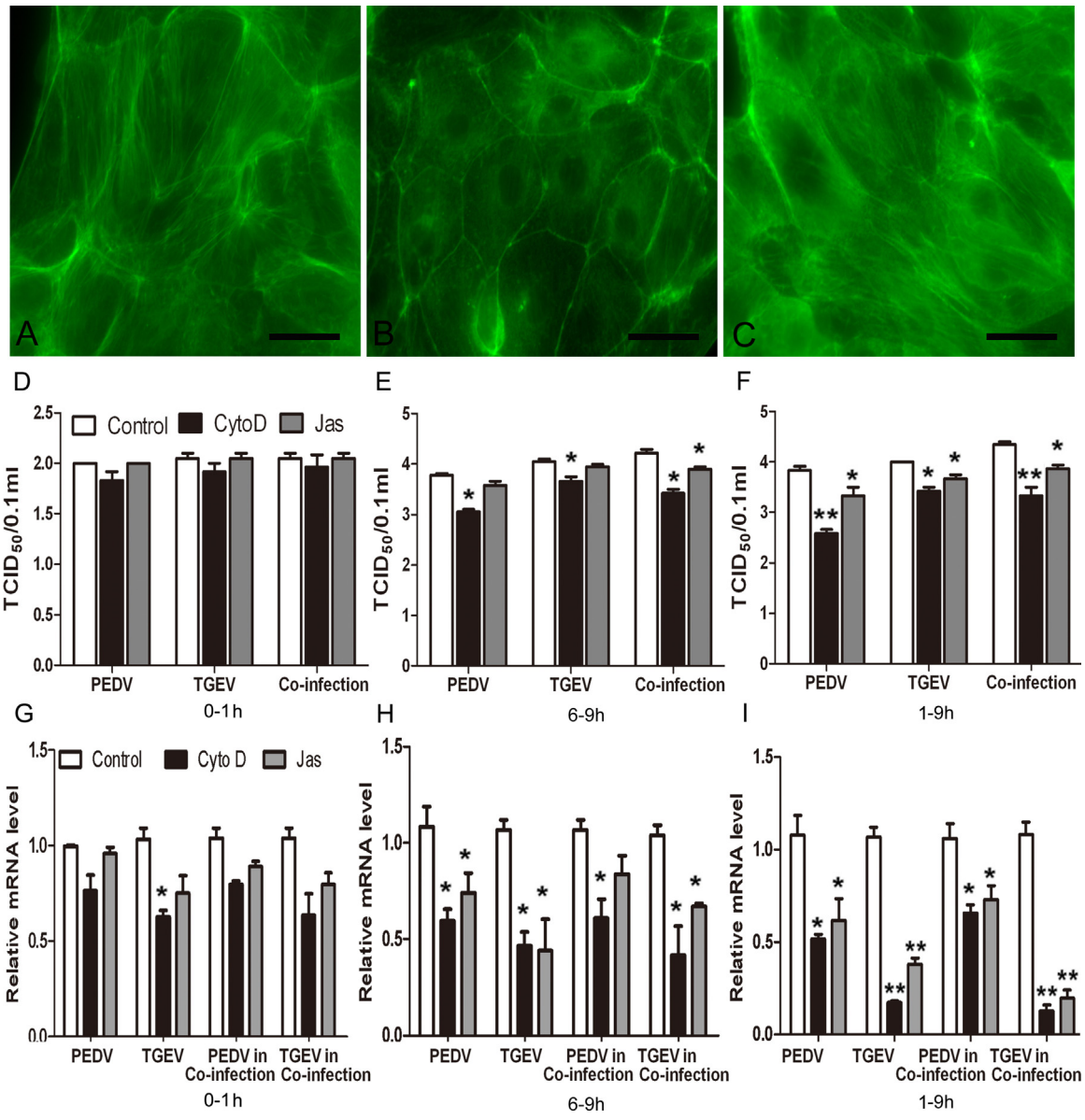

Fig. 4. Microfilaments are required for PEDV and TGEV replication and release. (A–C) Immunofluorescence images of microfilaments in PEDV and TGEV infected and mock IPEC-J2 cells which treated with or without treated with or without microfilaments inhibitors, Cytochalasin D and Jasplakinolide at 6 hpi were stained with FTTC-phalloidin. Scale bars represent 10 μm. (A) Immunofluorescence images of microfilaments of the mock IPEC-J2 cells were a complex three-dimensional network composed of microfilaments extending throughout the cell body. (B) Microfilaments of IPEC-J2 cells treated by Cytochalasin D were irregular and non-uniformly distributed throughout the cell. Some areas appeared to be completely devoid of filaments, whereas had formed the dense network aggregates, clumps, or even compact foci of filamentous materials at 6 hpi. (C) The microfilaments of IPEC-J2 cells treated by Jasplakinolide showed an increased density of microfilaments adjacent to the plasma membrane and cytoplasm at 6 hpi. The viral titres of PEDV and TGEV that entry (D), release (E), replication and release (F) from the IPEC-J2 cells treated with microfilaments inhibitor, Jasplakinolide and cytochalasin D were analysed by $TCID_{50}$. Data express the mean ± SEM ($n = 3$). The symbol * indicates statistically significant differences ($P < 0.05$) when compared with the control group, and the symbol ** indicates statistically very significant differences ($P < 0.01$) when compared with the control group. The viral M gene RNA relative level of PEDV and TGEV that entry (G), release (H), replication and release (I) from the IPEC-J2 cells treated with microfilaments inhibitor, Jasplakinolide and cytochalasin D were analysed by qRT-PCR. Data express the mean ± SEM ($n = 3$). The symbol * indicates statistically significant differences ($P < 0.05$) when compared with the control group, and the symbol ** indicates statistically very significant differences ($P < 0.01$) when compared with the control group.

3.4. PEDV and TGEV infection reorganised the microfilaments of IPEC-J2 cells

In order to assess how the PEDV, TGEV and PEDV + TGEV infection induced dramatic cytoskeletal reorganisation of the microfilaments, we used the FITC-Phalloidin to show filamentous actin in these infected IPEC-J2 cells. The control cells showed a complex three-dimensional network composed of microfilaments extending throughout the cell body (Fig. 3G, left). After 40 min of infection, the microfilaments were irregularly distributed throughout the cell. They dissolved in the PEDV-infected IPEC-J2 cells, and retracted and formed pronounced foci around certain membrane structures and the plasma membrane in the TGEV-infected and PEDV + TGEV-infected IPEC-J2 cells (Fig. 3G, the first line). After 1 h of infection, the bundles of microfilaments were found to line the plasma membrane in all virus-infected IPEC-J2 cells (Fig. 3G, the second line). The plasma membrane appeared to be completely devoid of filaments, whereas dense network aggregates, clumps, or even compact foci of filamentous material had formed in the nuclear membrane of all virus-infected IPEC-J2 cells at 12 hpi (Fig. 3G, the third line). After 24 h of infection, the microfilaments in the cytoplasm were more diffusely fluorescent, and retraction of

the microfilaments in a perinuclear location formed juxtanuclear caps or rings in their infected cells (Fig. 3G, the last line).

3.5. The effect of Jas and Cyto D on viral attachment, replication and release

In order to determine whether the microfilaments are required for PEDV and TGEV infection, we treated IPEC-J2 cells with Cyto D (Fig. 4B), which can induce destabilisation of the microfilaments, and Jas (Fig. 4C), which is able to promote microfilament stabilisation. First, the data showed that neither Jas nor Cyto D affected the ability of PEDV, TGEV and PEDV + TGEV to enter the IPEC-J2 cells ($p < 0.05$) (Fig. 4D, left). However, Cyto D notably inhibited all viral release from IPEC-J2 ($p < 0.05$), and the Jas group only inhibited viral release in the PEDV + TGEV co-infection group (Fig. 4D, middle). Finally, Cyto D and Jas treated IPEC-J2 cells significantly decreased the replication and release of all viruses, especially when using the Cyto D treatment ($p < 0.01$) (Fig. 4D, right). To further validate the effects of microfilament disorder on the attachment, replication and release of PEDV and TGEV, the qRT-PCR was used to detect the viral level. Form the results, only Cyto D could affect the ability of TGEV to enter the IPEC-J2 cells ($p < 0.05$) (Fig. 4G). Moreover, Jas and Cyto D notably inhibited all viral release from IPEC-J2 ($p < 0.05$) (Fig. 4H), and Cyto D and Jas treated IPEC-J2 cells significantly decreased the replication and release of all viruses, especially when using the Cyto D treatment ($p < 0.01$) (Fig. I). These results implied that microfilament disorder of IPEC-J2 cells did not affect the attachment of PEDV and TGEV, but inhibited the replication and release of them. Furthermore, microfilament depolymerisation in IPEC-J2 cells significantly affected the replication and release of PEDV and TGEV.

3.6. TGEV and PEDV infection affected the activation of MAPK signalling pathway in IPEC-J2 cells

The MAPK signalling pathway is not only able to modulate the expression of several TJ proteins, but also changes the microfilament remodelling in viral infection. From our results, the PEDV, TGEV and PEDV + TGEV infection resulted in a marked increase in the ratio of phospho-ERK1/2 and phospho-JNK in the IPEC-J2 cells at 60 minpi ($p < 0.05$), especially with regard to an increase in the intensity of phospho-JNK in TGEV infected IPEC-J2 cells ($p < 0.01$). However, the ratio of phosphor-p38 in the IPEC-J2 cells in all groups caused almost no alterations (Fig. 5A, left and 5B, up). In contrast, the PEDV, TGEV and PEDV + TGEV infection resulted in a notable decrease in the ratio of phospho-ERK1/2 and phospho-p38 in the IPEC-J2 cells ($p < 0.05$), but the phospho-JNK in all groups did not change at 24 hpi (Fig. 5A, right and 5B, down). Thus, these data demonstrate that PEDV, TGEV and their co-infection changed the levels of phospho-ERK1/2, phospho-p38 and phospho-JNK in IPEC-J2, and that the changes in tight junction and microfilaments of IPEC-J2 cells induced by TGEV and PEDV might be linked to activation of the MAPK signalling pathway.

3.7. The effects of MAPK pathway inhibitor on the infection of PEDV and TGEV, the tight junctions and microfilaments of IPEC-J2 cells

Since the changes of phospho-MAPKs were observed in PEDV and TGEV infection, the inhibitors of MAPKs (PD98059, SB203580 and SP600125) were employed to further investigate the role of the MAPKs in the infection of PEDV and TGEV, the tight junctions and microfilaments of IPEC-J2 cells. As we showed in Fig. 6A, inhibition of MAPKs failed to increase the viral replication. The ERK-MAPK-specific inhibitor (PD98059) and JNK-MAPK-specific inhibitor (SP600125) notably decreased the level of PEDV and TGEV infection at 12 hpi ($p < 0.05$) and 24 hpi ($p < 0.05$), and PD98059 extremely significantly inhibited the TGEV replication 24 hpi ($p < 0.01$), while p38-MAPK-specific inhibitor (SB203580) could not significantly inhibited the TGEV and PEDV replication ($p > 0.05$). These results indicated that MAPKs inhibitors, especially for ERK and JNK, were involved in PEDV and TGEV infection. From Fig. 6B, we could observed the PD98059 and SB203580 could significantly decreased the expression of E-cadherin and Occludin in the TGEV and PEDV infected IPEC-J2 cells at 12 hpi, and PD98059 also notably decreased the expression of E-cadherin, Occludin and Zo-1 in the TGEV and PEDV infected IPEC-J2 cells at 24 hpi. Moreover, SB203580 could suppress the expression of Claudin-1 in the TGEV and PEDV infected IPEC-J2 cells at 24 hpi. Thus, the results demonstrated that MAPKs inhibitors, especially for ERK and p38, could affect the expression of tight junctions of IPEC-J2 cells. Finally, the results from Fig. 6C and Additional Fig. 2 showed that inhibition of MAPKs significantly affected the microfilaments of IPEC-J2 cells. We observed that the microfilaments of IPEC-J2 cells treated with MAPKs inhibitors (PD98059, SB203580 and SP600125) disappeared in the cytoplasm or became more diffuse in the cytoplasm, then gathered in the plasma membrane after 40, 60 min and 12, 24 h of PEDV and TGEV infection. These results suggested that MAPKs inhibitors, ERK, p38 and JNK, were involved in the microfilaments of IPEC-J2 cells.

4. Discussion

PEDV and TGEV severely replicated in the intestinal epithelial cells of the newborn piglets, resulting in fatal diarrhoea. Because of the limited availability of epithelial cell lines of small intestinal origin, the knowledge concerning the interaction between intestinal epithelial cells and TGEV or PEDV is limited *in vitro*. IPEC-J2 cells was derived from jejunum epithelium isolated from the jejunum of un-suckled 12-hour-old piglets which formed an undifferentiated porcine intestinal epithelial cell line and was immortalised; therefore, it represented a better model of normal porcine intestinal epithelium than transformed cell lines (Liu et al., 2010). In the present study, we have indicated that both TGEV and PEDV can also infect IPEC-J2 cells. That might be that their common receptor (Aminopeptidase N) resides in IPEC-J2 cells.

The epithelial barrier is a critical border that segregates luminal material from entering tissues. Some viruses have developed specific strategies to alter or disrupt these structures as part of their pathogenesis, resulting in either viruses penetration, or other consequences such as diarrhoea (Coyne et al., 2007; Nava et al., 2004). Rotavirus decreases transepithelial electrical resistance (TEER) and increases paracellular permeability through decreased levels of claudin-1, occludin and ZO-1 proteins in the perijunctional region of Caco-2 monolayers; this was closely related to the fact that it caused viral astroenteritis leading to diarrhoea and morbidity in mammals (Nava et al., 2004). TGEV and PEDV also cause severe diarrhoea in piglets, whether this phenomenon is correlated to the damaged AJC in epithelial cells? Similarly, in our work, the expression of E-cadherin and ZO-1 were significantly reduced in the TGEV and PEDV + TGEV infected IPEC-J2 cells in early infection, while these four tight and adhesion junctions proteins unchanged in the TGEV and PEDV infected IPEC-J2 cells compared the control group in 24 hpi; therefore, the TEER of IPEC-J2 decreased and the permeability of IPEC-J2 increased, leading to the barrier integrity of IPEC-J2 cells undergoing temporary destruction. Subsequently, the barrier integrity returned to normal levels through self-repair over time. The rapid reduction of E-cadherin, occludin and ZO-1 in infection may be related to the virus internalisation. Previous reports have shown that adenoviruses-2 and -5 and Coxsackievirus use CAR as a receptor (Bergelson et al., 1997) for their internalisation

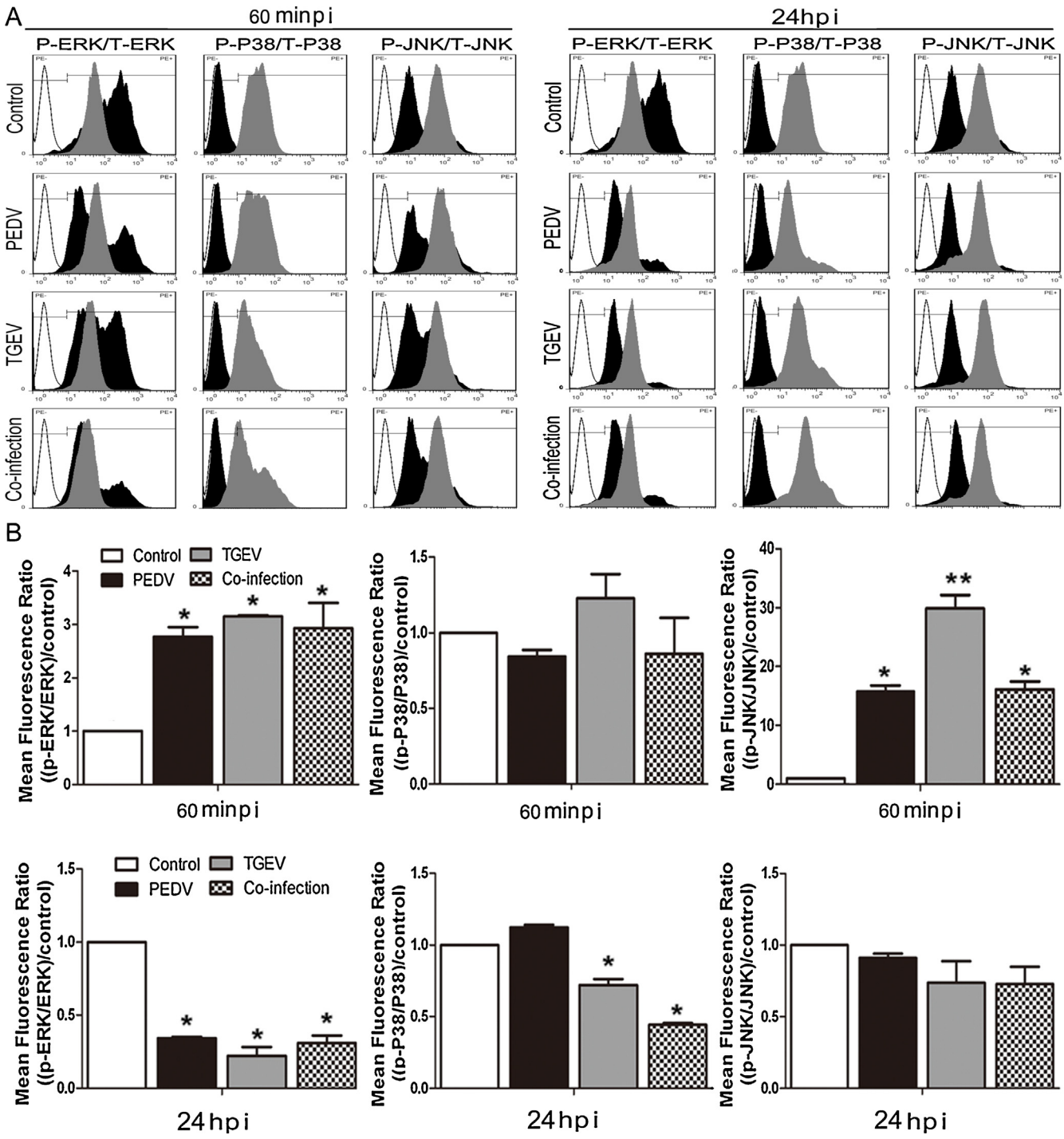

Fig. 5. PEDV and TGEV infection affected the activation of the MAPK signalling pathway in the IPEC-J2 cells. (A) Dot plots show the counts of ERK1/2, p38 and JNK in the PEDV-, TGEV-, and PEDV + TGEV-infected IPEC-J2 cells at 60 minpi (left) and 24 hpi (right). White histograms represent the negative control, black histograms represent phospho-proteins and grey histograms represent Total-proteins of ERK1/2, p38 and JNK in the infected cells. (B) Bar graphs show the relative rate of phospho-ERK1/2, phospho-p38 and phosphor-JNK in the PEDV-, TGEV-, and PEDV + TGEV-infected IPEC-J2 cells at 60 minpi (up) and 24 hpi (down). Data express the mean ± SEM ($n = 3$). The symbol * indicates statistically significant differences ($P < 0.05$) when compared with the control group, and the symbol ** indicates statistically very significant differences ($P < 0.01$) when compared with the control group.

and to break the epithelial barrier during viral escape. Whether the PEDV and TGEV use the AJC proteins as their receptor for their flexible invasion is not clear, but at least we observed that the epithelial barrier was destroyed in early viral infection. The expression of E-cadherin and ZO-1 were more reduced in the IPEC-J2 cells infected with TGEV and PEDV + TGEV than PEDV infection at 60 minpi probably because the virulence of TGEV is stronger than that of PEDV.

Multiple TJ components interact with the microfilaments (i.e., ZO-1/2/3, cingulin, and occludin) (Fanning et al., 2002). Regulation of the microfilaments and their interactions with TJ components play a major role in the infection of viruses. Furthermore, viruses use the host microfilament transport systems and their motors for several steps during their life cycle (Taylor et al., 2011). From our TEM results, during the infection of PEDV and TGEV, their attachment, internalisation, nuclear targeting, transport of progeny viral

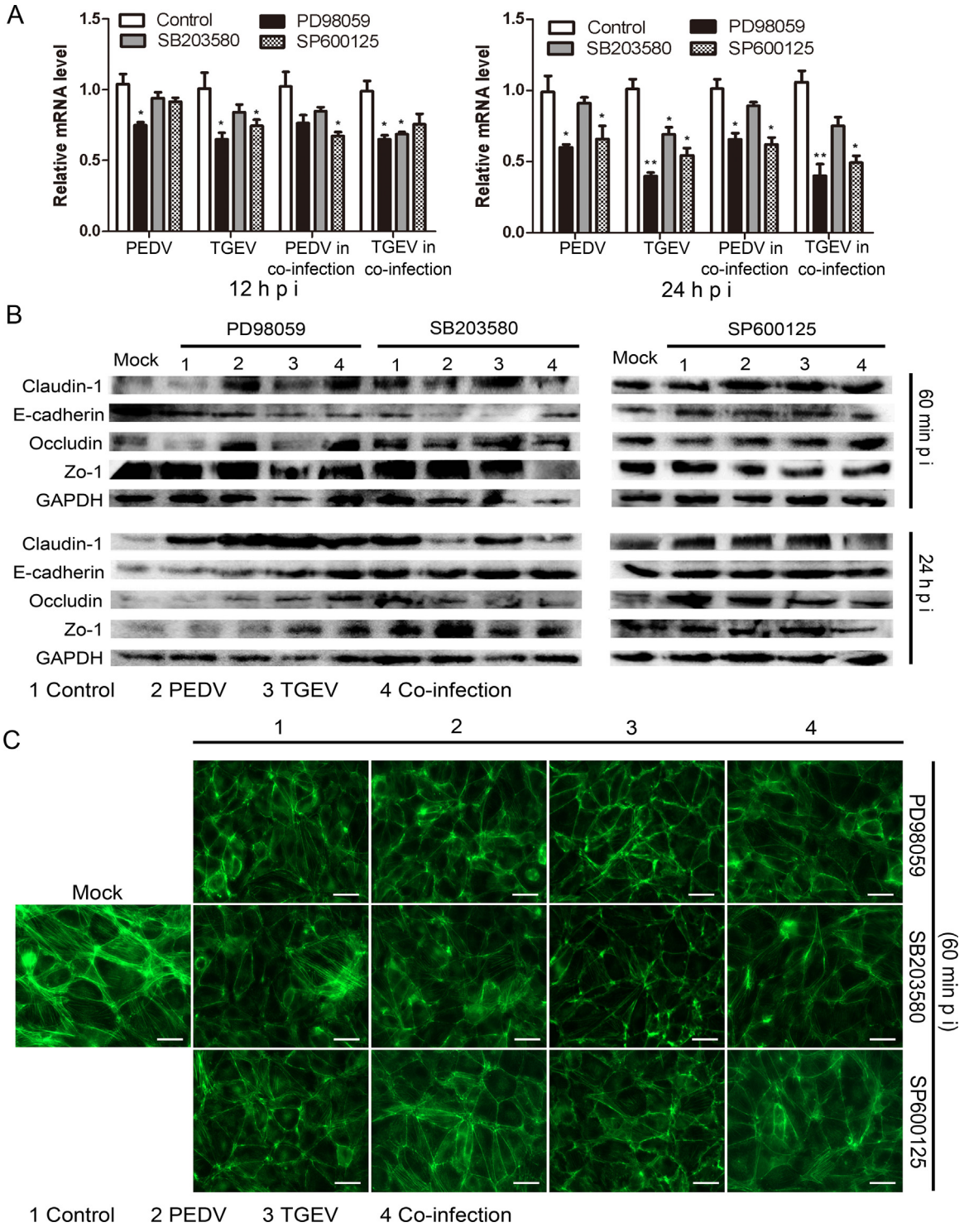

Fig. 6. The effects of MAPK pathway inhibitor on PEDV and TGEV infection, the tight junctions and microfilaments of IPEC-J2 cells. (A) The viral M gene RNA relative level of PEDV and TGEV in the IPEC-J2 cells treated with or without MAPKs inhibitors, PD98059, SB203580 and SP600125 were analysed by qRT-PCR. Data express the mean ± SEM ($n = 3$). The symbol * indicates statistically significant differences ($P < 0.05$) when compared with the control group, and the symbol ** indicates statistically very significant differences ($P < 0.01$) when compared with the control group. (B) The expression of Claudin-1, E-cadherin, Occludin and ZO-1 in PEDV and TGEV infected and mock IPEC-J2 cells which treated with or without MAPKs inhibitors, PD98059, SB203580 and SP600125 at 60 minpi and 24 hpi was analysed via western blotting. (C) Immunofluorescence images of microfilaments in PEDV and TGEV infected and mock IPEC-J2 cells which treated with or without treated with or without MAPKs inhibitors, PD98059, SB203580 and SP600125 at 60 minpi were stained with FTTC-phalloidin. Scale bars represent 10 μm. Immunofluorescence images of microfilaments of the mock IPEC-J2 cells were a complex three-dimensional network composed of microfilaments extending throughout the cell body. Microfilaments of IPEC-J2 cells treated by PD98059, SB203580 and SP600125 disappeared in the cytoplasm or became more diffuse in the cytoplasm, and gathered in the plasma membrane after 60 min of infecting PEDV and TGEV.

particles and release was shown to be assisted by the microfilaments during the viral campaign, suggesting that actin filaments play important roles in virus life cycles. However, the question of what changes in the distribution of microfilaments occurred during the process of viral infection remained? First, the microfilaments of PEDV- and TGEV-infected IPEC-J2 retracted and concentrated around certain membrane structures and the plasma membrane, which might indicate preparation for the adsorption and internalisation of the virus. Then, the bundles of microfilaments were seen to line the plasma membrane in infected IPEC-J2, which might indicate the attachment and internalisation of these viruses. Similarly, HIV, measles virus or herpes simplex virus also cause the microfilaments to concentrate around the plasma membrane for their attachment and internalisation (Döhner and Sodeik, 2005; Smith and Helenius, 2004). After internalisation, these viruses are transported inside vesicles to the cytosol for replication of their genome and protein synthesis. Subsequently, the subviral components are found to bud from the plasma membrane via disruption of this membrane, which frees all of the progeny. Thus, after 12 h of infection, the microfilaments appeared as numerous of spotting-like structures around the nuclear membrane in all virus-infected IPEC-J2 cells. These spotting-like structures might be the ER or the Golgi apparatus which were the site of viral genome replication and protein synthesis. The microfilaments then gradually located in the perinuclear area and the plasma membrane, and this may be an indication that these viruses were budding from the plasma membrane. These results implied that viruses can interfere with cytoskeleton and induce actin rearrangements, supporting infection. However, determination of whether those spotting-like structures were ER or Golgi apparatus requires further research.

To further validate the role of microfilaments in the viral life cycle, we treated IPEC-J2 cells with Jas, which promotes stabilisation of the microfilaments, and Cyto D, which induces destabilisation of the microfilaments. We found that neither stabilised nor depolymerised microfilaments affected the adsorption process of these viruses. That might be because the changes in the distribution of microfilaments did not decrease the number of viral receptors, but simply affected the speed of viral adsorption. However, microfilament disorder, either stabilisation or depolymerisation, could inhibit the replication and release of viruses, and in particular the depolymerisation of microfilaments. These results were consistent with a requirement of dynamic microfilaments for other viruses, such as Echovirus 11 and herpesvirus, among others (Forest et al., 2005; Sobo et al., 2012). However, it was not clear how these stabilised or depolymerised microfilaments affected the viral production and budding. The RNA genome of human parainfluenza virus type 3 is replicated and transcribed in association with ribonucleoproteins bound to microfilaments, and depolymerisation of microfilaments inhibits viral RNA synthesis (Gupta et al., 1998). Simpson-Holley reported that budding of the influenza virus is also affected by microfilament-depolymerising drugs, probably because the microfilament cortex maintains the correct structure of lipid rafts that are incorporated into the viral envelope (Simpson-Holley et al., 2002). The exact mechanisms why the microfilament depolymerisation or stabilisation inhibited the replication and release of PEDV and TGEV are still unclear and require further investigation.

In our work, the lowest TEER and the highest permeability of IPEC-J2 cells infected with PEDV, TGEV and PEDV + TGEV appeared at 60 minpi. Moreover, the ratio of phospho-ERK1 and phospho-JNK of IPEC-J2 cells significantly increased at the same time post-infection. However, we observed the opposite results at 24 hpi. A similar report showed that the HIV-1 Tat protein could trigger the disappearance of ZO-1 from cell–cell contact sites in brain endothelia due to ERK1/2 activation (András et al., 2005). Patrick indicated that TNF-α and IFN-γ could damage the epithelial barrier by down-regulating the expression of occludin and ZO-1 through activating ERK1/2and p38 in MDCK cells (Patrick et al., 2006). We speculated that TGEV- and PEDV-damaged barrier function of IPEC-J2 cells may be related to the phospho-ERK1/2 and phospho-38 of the MAPK pathway activation. The ERK and p38 inhibitors significantly decreased the expression of the E-cadherin, Occludin and Zo-1 in the TGEV and PEDV infected IPEC-J2 cells, which indicated that activation of ERK and p38 probably involved in the damage of barrier function of IPEC-J2 cells when IPEC-J2 cells were infected with PEDV and TGEV. Moreover, the MAPK pathway also plays an important role in microfilaments remodelling. After 1 h of infection, the microfilaments were found to line in the plasma membrane among all virus-infected IPEC-J2 cells. Simultaneously, the ratio of phospho-ERK1/2 and phospho-JNK in these viruses infected IPEC-J2 cells significantly increased. After 24 h of infection, the microfilaments in a perinuclear location formed juxtanuclear caps or rings, while the phospho-ERK1/2 and phospho-38 in the infected IPEC-J2 cells significantly decreased. In endothelial cells, p38 MAPK is reported to activate MAPK-activated protein (MAPKAP) kinase 2, which phosphorylates the 27 kDa heat shock protein (HSP27), an F-actin cap binding protein, which causes actin depolymerisation (Kutsuna et al., 2004). SARS-CoV N protein also activates the p38 MAPK pathway to induce the reorganisation of microfilaments in cells devoid of growth factors (Surjit et al., 2004). TGEV- and PEDV-induced microfilament modelling might be due to the activation or inactivation of phospho-ERK1/2 and phospho-38 in the MAPK pathway. Using the MAPKs inhibitors to treat with the IPEC-J2 cells, the microfilaments of cells disappeared in the cytoplasm or became more diffuse in the cytoplasm, then gathered in the plasma membrane after 40, 60 min and 12, 24 h of PEDV and TGEV infection. These results suggested that MAPKs inhibitors, ERK, p38 and JNK, were involved in the microfilaments of IPEC-J2 cells. In addition, inhibition of MAPKs also decreased the PEDV and TGEV infection, which was consistent with the report that the effect of MAPK pathway inhibitors on HIV infection (Gong et al., 2011). However, the relationship between the PEDV and TGEV infection and MAPK pathway remains to be further investigated.

Conflict of interest statement

The authors declare that they have no competing interests.

Acknowledgements

This work was supported by Grant number 31372465 from the National Science Grant of China, and another project funded by the Priority Academic Program Development (PAPD) of Jiangsu Higher Education Institutions.

Appendix A. Supplementary data

Supplementary data associated with this article can be found, in the online version, at http://dx.doi.org/10.1016/j.virusres.2014.08.014.

References

András, I.E., Pu, H., Tian, J., Deli, M.A., Nath, A., Hennig, B., Toborek, M., 2005. Signaling mechanisms of HIV-1 Tat-induced alterations of claudin-5 expression in brain endothelial cells. J. Cereb. Blood Flow Metab. 25, 1159–1170.

Avota, E., Gassert, E., Schneider-Schaulies, S., 2011. Cytoskeletal dynamics: concepts in measles virus replication and immunomodulation. Viruses 3, 102–117.

Bergelson, J.M., Cunningham, J.A., Droguett, G., Kurt-Jones, E.A., Krithivas, A., Hong, J.S., Horwitz, M.S., Crowell, R.L., Finberg, R.W., 1997. Isolation of a common receptor for Coxsackie B viruses and adenoviruses 2 and 5. Science 275, 1320–1323.

Brian, D.A., Baric, R., 2005. Coronavirus genome structure and replication. In: Coronavirus Replication and Reverse Genetics. Springer, New York, pp. 1–30.

Burckhardt, C.J., Greber, U.F., 2009. Virus movements on the plasma membrane support infection and transmission between cells. PLoS Pathog. 5, e1000621.

Cereijido, M., Contreras, R.G., Shoshani, L., Flores-Benitez, D., Larre, I., 2008. Tight junction and polarity interaction in the transporting epithelial phenotype. Biochim. Biophys. Acta 1778, 770–793.

Chae, C., Kim, O., Choi, C., Min, K., Cho, W.S., Kim, J., Tai, J.H., 2000. Prevalence of porcine epidemic diarrhoea virus and transmissible gastroenteritis virus infection in Korean pigs. Vet. Rec. 147, 606–608.
Coyne, C.B., Shen, L., Turner, J.R., Bergelson, J.M., 2007. Coxsackievirus entry across epithelial tight junctions requires occludin and the small GTPases Rab34 and Rab5. Cell Host Microbe 2, 181–192.
Döhner, K., Sodeik, B., 2005. The role of the cytoskeleton during viral infection. In: Membrane Trafficking in Viral Replication. Springer, New York, pp. 67–108.
Etournay, R., Zwaenepoel, I., Perfettini, I., Legrain, P., Petit, C., El-Amraoui, A., 2007. Shroom2, a myosin-VIIa- and actin-binding protein, directly interacts with ZO-1 at tight junctions. J. Cell Sci. 120, 2838–2850.
Evans, M.J., von Hahn, T., Tscherne, D.M., Syder, A.J., Panis, M., Wolk, B., Hatziioannou, T., McKeating, J.A., Bieniasz, P.D., Rice, C.M., 2007. Claudin-1 is a hepatitis C virus co-receptor required for a late step in entry. Nature 446, 801–805.
Fanning, A.S., Ma, T.Y., Anderson, J.M., 2002. Isolation and functional characterization of the actin binding region in the tight junction protein ZO-1. FASEB J. 16, 1835–1837.
Forest, T., Barnard, S., Baines, J.D., 2005. Active intranuclear movement of herpesvirus capsids. Nat. Cell Biol. 7, 429–431.
Gerits, N., Mikalsen, T., Kostenko, S., Shiryaev, A., Johannessen, M., Moens, U., 2007. Modulation of F-actin rearrangement by the cyclic AMP/cAMP-dependent protein kinase (PKA) pathway is mediated by MAPK-activated protein kinase 5 and requires PKA-induced nuclear export of MK5. J. Biol. Chem. 282, 37232–37243.
Gong, J., Shen, X.H., Chen, C., Qiu, H., Yang, R.G., 2011. Down-regulation of HIV-1 infection of the MAPK signaling pathway. Virol. Sin. 26, 114–122.
Gonzalez-Mariscal, L., Tapia, R., Chamorro, D., 2008. Crosstalk of tight junction components with signaling pathways. Biochim. Biophys. Acta 1778, 729–756.
Guglielmi, K.M., Kirchner, E., Holm, G.H., Stehle, T., Dermody, T.S., 2007. Reovirus binding determinants in junctional adhesion molecule-A. J. Biol. Chem. 282, 17930–17940.
Gupta, S., De, B.P., Drazba, J.A., Banerjee, A.K., 1998. Involvement of actin microfilaments in the replication of human parainfluenza virus type 3. J. Virol. 72, 2655–2662.
He, K.W., Li, J.H., Huan, H., Ni, Y.X., Qian, Y.Q., He, J.H., Hou, J., 2001. Studies on cell cultivation and pathogenicity of attenuated transmissible gastroenteritis virus STC3. Chin. J. Vet. Sci. Technol. 31, 8–10.
Hofmann, M., Wyler, R., 1988. Propagation of the virus of porcine epidemic diarrhea in cell culture. J. Clin. Microbiol. 26, 2235–2239.
Kim, O., Chae, C., 2003. Experimental infection of piglets with a Korean strain of porcine epidemic diarrhoea virus. J. Comp. Pathol. 129, 55–60.
Kim, O., Chae, C., Kweon, C.H., 1999. Monoclonal antibody-based immunohistochemical detection of porcine epidemic diarrhea virus antigen in formalin-fixed, paraffin-embedded intestinal tissues. J. Vet. Diagn. Invest. 11, 458–462.
Kutsuna, H., Suzuki, K., Kamata, N., Kato, T., Hato, F., Mizuno, K., Kobayashi, H., Ishii, M., Kitagawa, S., 2004. Actin reorganization and morphological changes in human neutrophils stimulated by TNF, GM-CSF, and G-CSF: the role of MAP kinases. Am. J. Physiol. Cell Physiol. 286, C55–C64.
Liu, F., Li, G., Wen, K., Bui, T., Cao, D., Zhang, Y., Yuan, L., 2010. Porcine small intestinal epithelial cell line (IPEC-J2) of rotavirus infection as a new model for the study of innate immune responses to rotaviruses and probiotics. Viral Immunol. 23, 135–149.
McBride, C.E., Machamer, C.E., 2010. Palmitoylation of SARS-CoV S protein is necessary for partitioning into detergent-resistant membranes and cell-cell fusion but not interaction with M protein. Virology 405, 139–148.
Melamed, I., Franklin, R.A., Gelfand, E.W., 1995. Microfilament assembly is required for anti-IgM dependent MAPK and p90rsk activation in human B lymphocytes. Biochem. Biophys. Res. Commun. 209, 1102–1110.
Nava, P., López, S., Arias, C.F., Islas, S., González-Mariscal, L., 2004. The rotavirus surface protein VP8 modulates the gate and fence function of tight junctions in epithelial cells. J. Cell Sci. 117, 5509–5519.
Patrick, D., Leone, A., Shellenberger, J., Dudowicz, K., King, J., 2006. Proinflammatory cytokines tumor necrosis factor-and interferon-modulate epithelial barrier function in Madin–Darby canine kidney cells through mitogen activated protein kinase signaling. BMC Physiol. 6, 2.
Pontefract, R.D., Ng, C.W., Bergeron, G., 1989. Vero cells co-infected with *Chlamydia trachomatis* and herpes simplex virus type 2: a scanning and transmission electron microscope study. Sex. Transm. Dis. 16, 74–78.
Sestak, K., Saif, L.J., 2002. Porcine Coronaviruses – Trends in Emerging Viral Infections of Swine. Section 10., pp. 321.
Shatos, M.A., Doherty, J.M., Orfeo, T., Hoak, J.C., Collen, D., Stump, D.C., 1992. Modulation of the fibrinolytic response of cultured human vascular endothelium by extracellularly generated oxygen radicals. J. Biol. Chem. 267, 597–601.
Simpson-Holley, M., Ellis, D., Fisher, D., Elton, D., McCauley, J., Digard, P., 2002. A functional link between the actin cytoskeleton and lipid rafts during budding of filamentous influenza virions. Virology 301, 212–225.
Smith, A.E., Helenius, A., 2004. How viruses enter animal cells. Science 304, 237–242.
Sobo, K., Stuart, A.D., Rubbia-Brandt, L., Brown, T.D.K., McKee, T.A., 2012. Echovirus 11 infection induces dramatic changes in the actin cytoskeleton of polarized Caco-2 cells. J. Gen. Virol. 93, 475–487.
Surjit, M., Liu, B., Jameel, S., Chow, V., Lal, S., 2004. The SARS coronavirus nucleocapsid protein induces actin reorganization and apoptosis in COS-1 cells in the absence of growth factors. Biochem. J. 383, 13–18.
Taylor, M.P., Koyuncu, O.O., Enquist, L.W., 2011. Subversion of the actin cytoskeleton during viral infection. Nat. Rev. Microbiol. 9, 427–439.
Vaughan, J.C., Brandenburg, B., Hogle, J.M., Zhuang, X., 2009. Rapid actin-dependent viral motility in live cells. Biophys. J. 97, 1647–1656.